

# The Abrasive Wear Properties of Al-Mg-Si<sub>3</sub>N<sub>4</sub> Metal Matrix Composites

Wang Shou-Ren, Geng Hao-Ran, Wang Ying-Zi, and Sun Bin

(Submitted July 28, 2005; in revised form December 1, 2005)

**One kind of three-dimensional network structure, reinforced aluminum magnesium matrix composites, has been prepared by pressure-assisted and vacuum-driven infiltration technology. The composites interpenetrated with ceramic have higher wear resistance than the metal matrix owing to their special topology structure. The reinforcement volume fraction has a large effect on abrasive wear. The wear rate decreases with the increase of the volume fraction of reinforcement and increases with the increase of sliding time and applied load. The wear mechanism of the composites (abrasive wear) differs greatly from the matrix alloy (adhesive wear).**

**Keywords** Al-Mg matrix composites, ceramic, friction and wear, infiltration, three-dimensional network structure

## 1. Introduction

It is well known that the abrasive wear of metal matrix composites (MMC) has been found to be significantly lower than that of the matrix (Ref 1). Indeed, wear resistance can generally be enhanced by introducing a secondary phase into the matrix (Ref 2). The secondary phase used to strengthen MMCs can have several morphologies: particles, whisker, or fibers (Ref 3-5). The wear properties of MMCs can be varied substantially through changes in the microstructure, the morphology, volume fraction, and the mechanical properties of the secondary phase. Specifically, the wear resistance of MMCs increases distinctly with the increase in the volume fraction of secondary phase for a range of 0 to 0.5. However, it is difficult to manufacture MMCs reinforced by high-volume fractions of secondary phases due to void formation resulting from imperfect wetting and agglomeration (Ref 2). Generally speaking, wear represents one of the tremendous and unavoidable losses in engineering. So the research of new wear-resistance materials continues to be an important task in which many researchers are interested. In recent years, three-dimensional (3-D) network structures, ceramic reinforced MMCs (3DNCRMMC), have received much attention due to their good wear resistance (Ref 6, 7). The 3DNCRMMCs have a special topology structure (i.e., ductile and brittle phases interpenetrating and intertwining) to overcome the problem of particle reinforcement agglomeration and asymmetry of whisker and fiber reinforcement. As such, the wear behavior of 3DNCRMMCs is unique, but little work has been carried out on the friction and abrasive wear properties of 3DNCRMMCs. The abrasive wear mecha-

nism for 3DNCRMMCs has unusual characteristics due to its special 3-D topological structure. So, research into the friction and wear behavior of 3DNCRMMCs has a great deal of significance.

## 2. Experimental Procedure

### 2.1 Fabrication of Si<sub>3</sub>N<sub>4</sub>-Al-Mg Metal Matrix Composites

A reticulated polyurethane (PU) with interconnected pores was chosen as a template to prepare the porous preform using the replica technology. The pore size of the PU was approximately 1 to 3 mm (or 5-10 pores per in.). A 99.4wt.%Si<sub>3</sub>N<sub>4</sub> powder was used as the starting material with sintering additives of 5wt.%Al<sub>2</sub>O<sub>3</sub>, 5wt.%ZrO<sub>2</sub>, and 5wt.%Al fine powder. These additives were mixed with the starting material and ball-milled for 4 h using Al<sub>2</sub>O<sub>3</sub> balls. The mixed slurry was stirred and immersed into the preceramic materials. The preform was sintered in a furnace in air. The sintering temperature was 1400 °C with a heating rate of 200 °C/h. The morphology of the reticulated Si<sub>3</sub>N<sub>4</sub> ceramic preform after immersing and sintering is shown in Fig. 1.

The raw metals used in this research are Al (ingot form 99.7% by weight) and Mg (ingot form 99.95% by weight), which were melted in a furnace for infiltration into the preform. The chemical composition of the Al-Mg alloy is shown in Table 1. The porous Si<sub>3</sub>N<sub>4</sub> ceramic skeleton was heated in a furnace under a nitrogen atmosphere until the desired temperature for processing was reached, at which point the liquid metal was infiltrated into the preform with the help of pressure and vacuum. A sketch of infiltration equipment is shown in Fig. 2.

The microstructural characterization of 3DNCRMMCs was performed with a scanning electron microscope (SEM) (model No. S-2500, Hitachi, Tokyo, Japan). Figure 3 shows a region marked "1," which is the Si<sub>3</sub>N<sub>4</sub> skeleton. The region marked "2" corresponds to the metal matrix. The mechanical properties of the Al-Mg alloy and the Al-Mg-Si<sub>3</sub>N<sub>4</sub> composites are shown in Table 2.

### 2.2 The Friction and Wear Experiment

The wear specimens were tested under dry conditions. The wear apparatus is illustrated schematically in Fig. 4. Test

**Wang Shou-Ren**, The Key Laboratory of Liquid Structure and Heredity of Materials of Shandong University, Jinan, China 250014; **Sun Bin**, School of Mechanical Engineering, and **Geng Hao-Ran** and **Wang Ying-Zi**, School of Material Science, Jinan University, Jinan, China 250022. Contact e-mail: strong\_422@163.com.

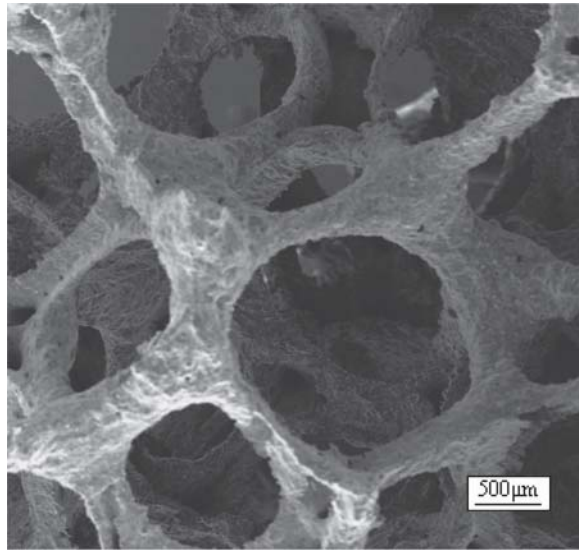


Fig. 1 Morphology of Si<sub>3</sub>N<sub>4</sub> reticulated ceramics

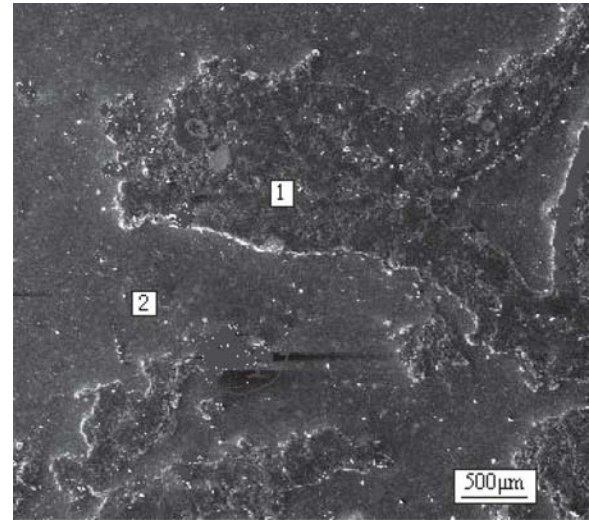


Fig. 3 SEM micrographs of the Al-Mg-Si<sub>3</sub>N<sub>4</sub> composite

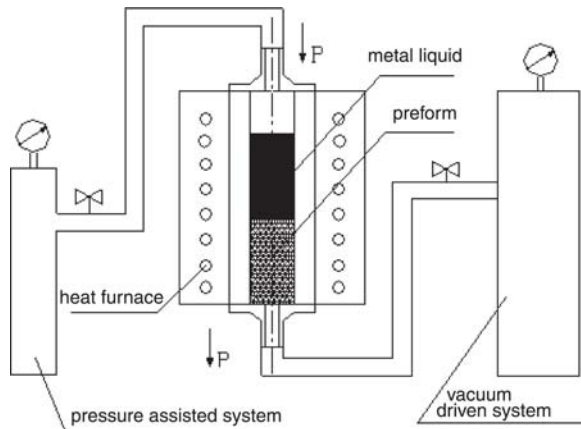


Fig. 2 Schematic diagram of infiltration equipment

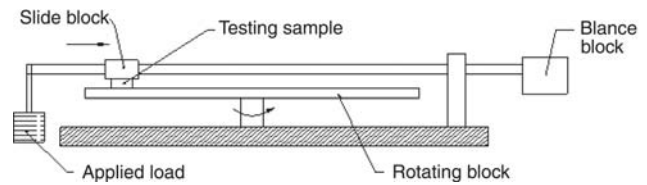


Fig. 4 Schematic diagram of wear test apparatus

Table 1 Chemical compositions of Al-Mg alloy (wt.%)

Mg	Fe	Si	Mn	Zn	Ti	Cr	Al
5.56	0.02	0.15	0.066	0.02	0.02	0.01	bal

samples were machined to 15 × 15 × 10 mm. The applied loads were 25, 50, 75, 100, 125, and 150 N, respectively. The rotating velocity of the steel disk was 1400 revolutions/min with test times of 5, 10, 15, and 20 min, corresponding to sliding distances of 200, 400, 600, and 800 m, respectively. The test samples were degreased and cleaned with an alcohol solution prior to testing. Alumina abrasive paper (360-grit corresponding to a nominal alumina particle size of 60 μm) covered the friction disk. To prevent wear debris from the specimen from clogging the abrasive paper, and to reduce the magnitude of mass loss gradually over time, a “slide” block translated the test sample in a direction perpendicular to the rotating velocity. Each test was concluded when the life of abrasive paper was exhausted. All conditions of the tribological tests are compiled in Table 3.

Table 2 Properties of Al-Mg-Si<sub>3</sub>N<sub>4</sub> composites and Al-Mg alloy

Material	Elastic modulus, GPa	HRB	Elongation, %	UTS, MPa	Density, g/cm <sup>3</sup>
Al-Mg alloy	66	65	7.5	303	2.66
Al-Mg-12Si <sub>3</sub> N <sub>4</sub>	87	71	3.2	315	2.78
Al-Mg-18Si <sub>3</sub> N <sub>4</sub>	84	78	2.2	298	2.98
Al-Mg-25Si <sub>3</sub> N <sub>4</sub>	70	84	1.6	290	3.11

Table 3 Parameters for friction and wear experiment

Counter-body: abrasive disk-diameter = 5 mm	Motion type: rotational sliding
No. of cycles: 1400 rotations/min	Surrounding environment: air
Relative humidity: 30 ~ 50%	Sample size: 15 × 15 × 10 mm
Applied load <i>P</i> : 25, 50, 75, 100, 125, 150 N	Lubricant: none
Temperature: 22 °C	Sliding distance: 200, 400, 600, 800 m

## 3. Results and Discussion

### 3.1 Wear Properties

The abrasive wear resistance of Al-Mg-Si<sub>3</sub>N<sub>4</sub> composites is significantly better than that of single-phase materials. The wear processes in Al-Mg-Si<sub>3</sub>N<sub>4</sub> composites are more complex than those in the single-phase metal. The reinforcement volume fraction has a large effect on abrasive wear, which can be seen in Fig. 5. The volume loss of the alloy sample without reinforcement increases rapidly with the increase in test time (slid-

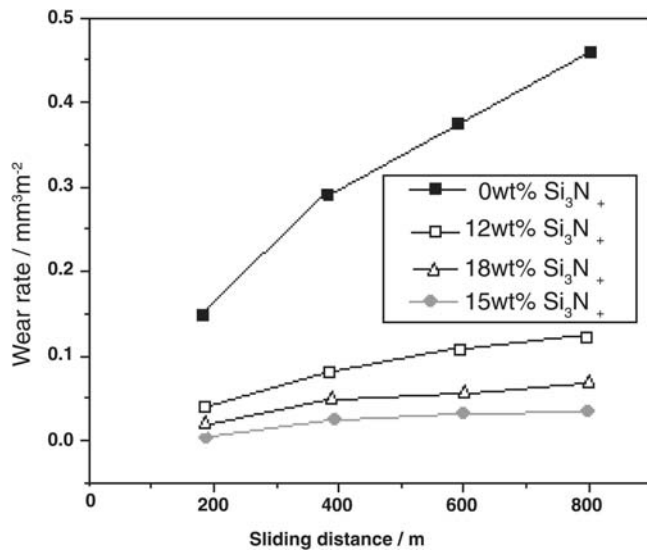


**Fig. 5** Effect of the wt.% of Si<sub>3</sub>N<sub>4</sub> on the wear rate for different wear times (applied load 50 N)

ing distance), and then the volume loss decreases at a lower rate. This arises for two reasons: the cutting edges of the alumina are damaged during the test; and the space between the abrasive particles fills up with wear debris. For the Al-Mg-Si<sub>3</sub>N<sub>4</sub> composites, the volume loss also increases with the increase in test duration (with test time corresponding to sliding distance). Volume loss in the Al-Mg-Si<sub>3</sub>N<sub>4</sub> composites is much less than that in the alloy. The volume loss for the composites decreases with the increase in the content of the Si<sub>3</sub>N<sub>4</sub> phase. The mass loss of the alloy is 0.51 g for a sliding distance of 200 m, but was 1.37 g for a sliding distance of 800 m. The mass loss for the Al-Mg-25 wt.% Si<sub>3</sub>N<sub>4</sub> composite is 0.02 g for a sliding distance of 200 m, and only 0.05 g for a sliding distance of 800 m.

The applied load has a large influence on the wear of the metal matrix and the Al-Mg-Si<sub>3</sub>N<sub>4</sub> composites. From Fig. 6, the wear volume loss for all materials increases with the increase in applied load. The volume loss is linear with applied load. As the volume fraction of ceramic increases, the volume loss decreases relative to the other composites. The volume loss for the Al-Mg-25 wt.% Si<sub>3</sub>N<sub>4</sub> composite is the smallest, with the other materials trending with the reinforcement fraction. The high hardness of the composites is directly related to the improved wear rate. Figure 7 shows the relationship between Rockwell hardness and the volume fraction of the ceramic phase in the composite. In Fig. 7, it is observed that hardness increases with the increase in the volume fraction of reinforcement in the composite.

### 3.2 Morphology of Wear Surface

With an increase in test time, the morphology of the worn surface changes from fine scratches to distinct grooves, which is an indication of severe surface damage. The worn surfaces of the alloy and the Al-Mg-Si<sub>3</sub>N<sub>4</sub> composites are shown in Fig. 8. Wear in the form of local damage, and even fractured flakes, is observed on the alloy wear surface. However, these same features are not observed in the Al-Mg-Si<sub>3</sub>N<sub>4</sub> composites, confirming the beneficial effect of the Si<sub>3</sub>N<sub>4</sub> network structure. From an examination of Fig. 8(a), the alloy exhibits distinct abrasive wear morphology, having deep and symmetrical furrows (Ref 8). The microstructure of the worn Al-Mg-Si<sub>3</sub>N<sub>4</sub>

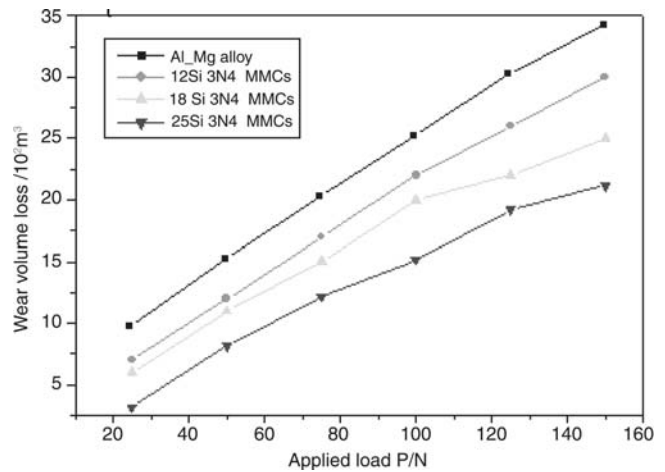


**Fig. 6** Wear volume loss as a function of applied load (wear test time 20 min, equivalent to a sliding distance of 800 m)

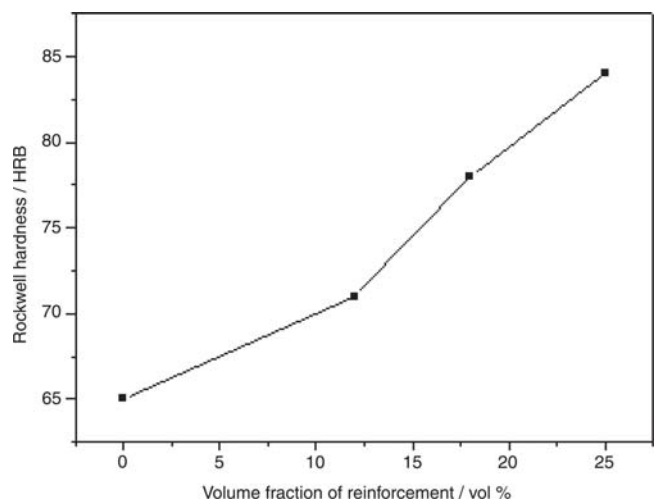
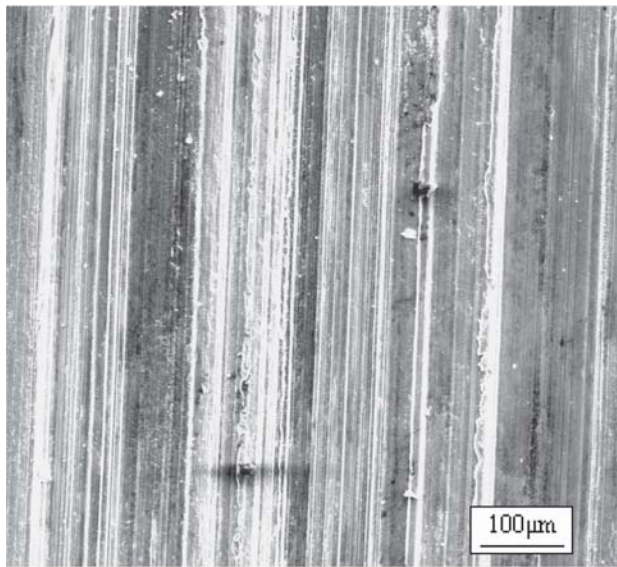


**Fig. 7** Relationship between Rockwell hardness and the volume fraction of reinforcement

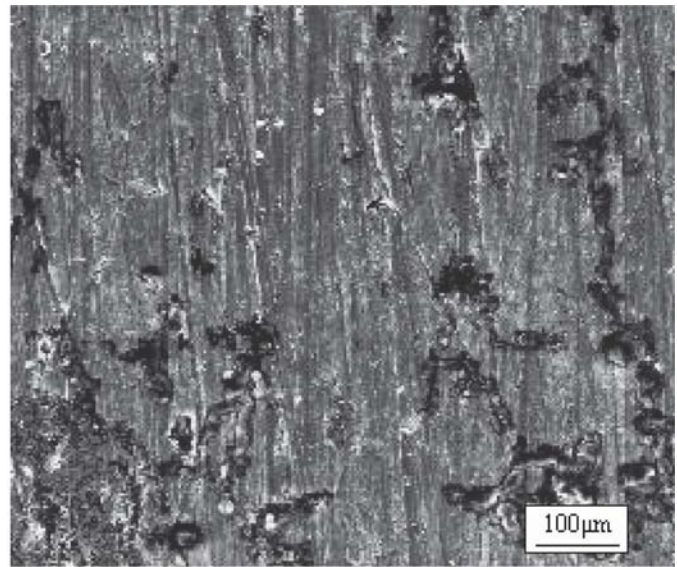
composites differs significantly. In general, the wear resistance of the Al-Mg-Si<sub>3</sub>N<sub>4</sub> composites increases with increasing Si<sub>3</sub>N<sub>4</sub> content. The width and depth of the wear grooves of the Al-Mg-Si<sub>3</sub>N<sub>4</sub>-12 wt.% composites are narrower and shallower than those of the matrix alloy (Fig. 8). The grooves become even more indistinct with the increasing Si<sub>3</sub>N<sub>4</sub> content. As the content increases, damage is more typically caused by grains fracturing and then breaking away from the Si<sub>3</sub>N<sub>4</sub> phase (Fig. 8c). The 25 wt.% Si<sub>3</sub>N<sub>4</sub> ceramic skeleton with the 3-D network structure has high stiffness and is very strong, forming a high-strength skeleton for the matrix alloy and reducing the contact area between the matrix and the abrasive paper. Thus, the Al-Mg-Si<sub>3</sub>N<sub>4</sub>-25 wt.% composites (Fig. 8d) have excellent wear resistance. The friction pair for the 3DNCrMMCs-abrasive is a classic hard-hard material combination, so the material removal mechanism differs greatly from that of the matrix alloy (i.e., a hard-soft material combination) (Ref 2).

## 4. Conclusions

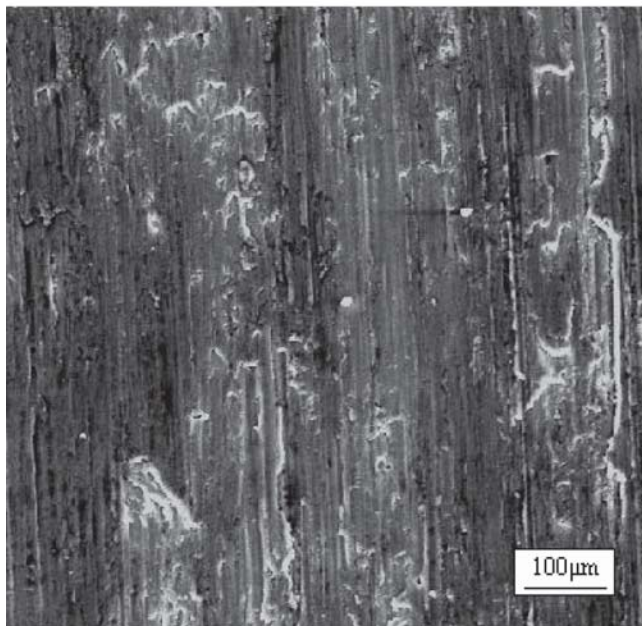
One kind of 3-D network structure-reinforced aluminum magnesium matrix composites has been prepared via melt infiltration technology using a pressure-assisted vacuum melting



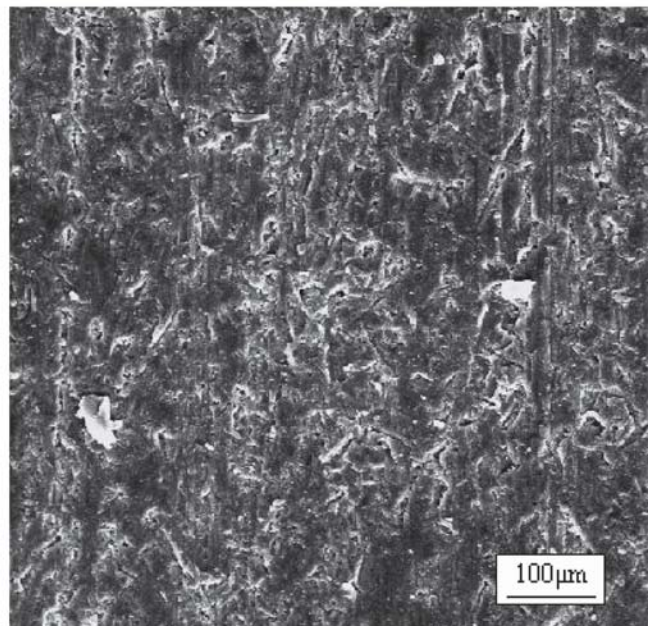
(a)



(b)



(c)



(d)

**Fig. 8** The microstructure of the wear surfaces of (a) the Al-Mg alloy, (b) the Al-Mg-Si<sub>3</sub>N<sub>4</sub>-12 wt.% composite, (c) the Al-Mg-Si<sub>3</sub>N<sub>4</sub>-18 wt.% composite, and (d) the Al-Mg-Si<sub>3</sub>N<sub>4</sub>-25 wt.% composite (25 N load; 20 min test duration or 800 m sliding distance)

furnace. The 3DNCRMMCs have better wear resistance than the matrix alloy. The reinforcement volume fraction has a large effect on abrasive wear. The 3-D ceramic structure in the matrix reduces the wear, and the volume wear decreases with an increase in the volume fraction of reinforcement.

### Acknowledgment

Project (50,371,047) was supported by the National Natural Science Foundation of China.

### References

1. A.C. McGee, C.K.H. Dharan, and I. Finnie, Abrasive Wear of Graphite Fiber-Reinforced Polymer Composites Materials, *Wear*, 1987, **114**, p 97-107
2. G.Y. Lee, C.K.H. Dharan, and R.O. Ritchie, A Physically-Based Abrasive Wear Model for Composites Materials, *Wear*, 2002, **252**, p 322-331
3. H.Y. Wang, Q.C. Jiang, and Y.Q. Zhao, Fabrication of TiB<sub>2</sub> and TiB<sub>2</sub>-TiC Particulates Reinforced Magnesium Matrix Composites, *Mater. Sci. Eng., A*, 2004, **372**, p 109-114
4. Z. Trojanova, P. Lukac, W. Riehemann, and B.L. Mordike, Study of Relaxation of Residual Internal Stress in Mg Composites by Internal Friction, *Mater. Sci. Eng., A*, 2002, **324**, p 122-126
5. A.U. Xu, Z.R. Chawla, K.K. Wolfenden, A. Neuman, A. Liggett, and G.M. Chawla, Stiffness Loss and Density Decrease Due to Thermal Cycling in an Alumina Fiber/Magnesium Alloy Composite, *Mater. Sci. Eng., A*, 1995, **203**, p 75-80
6. K. Konopka, A. Olszówka-Myalska, and M. Szafran, Ceramic-Metal Composites with an Interpenetrating Network, *Mater. Chem. Phys.*, 2003, **81**, p 329-332
7. W.A.N.G. Shou-ren, G.E.N.G. Hao-ran, and L.I. Hai-gu, Fabrication and Progress of PIA About the Reticulated Ceramics Reinforcement in MMCs, *J. Jinan Univ. (Sci. & Tech.)*, 2005, **19**(3), p 197-200
8. I.M. Hutchings, Ductile-Brittle Transitions and Wear Maps for the Erosion and Abrasion of Brittle Materials, *J. Phys. D Appl. Phys.*, 1992, **25**, p 212-221